MNE 19 (2023) 100190

Contents lists available at ScienceDirect

Micro and Nano Engineering

journal homepage: www.sciencedirect.com/journal/micro-and-nano-engineering

Fully 3D-printed PVDF-TrFE based piezoelectric devices with PVDF-TrFE-rGO composites as electrodes

Antrea Spanou [a,b,c,*], Cecilia Persson [c], Stefan Johansson [a]

[a] Division of Microsystems Technology, Department of Materials Science and Engineering, Uppsala University, Uppsala 751 05, Sweden
[b] Graphmatech AB, Uppsala 753 18, Sweden
[c] Division of Biomedical Engineering, Department of Materials Science and Engineering, Uppsala University, Uppsala 751 05, Sweden

ARTICLE INFO

Keywords:
3D printing
Direct ink writing
rGO
PVDF-TrFE
Piezoelectric
Sensors
Actuators
Graphene
Additive manufacturing

ABSTRACT

Direct ink writing (DIW) is a promising additive manufacturing (AM) technique in the field of microsystems technology due to the potential for high detail resolution and the wide choice of materials suitable for the technique. In this study, inks of polyvinylidene fluoride-trifluoroethylene (PVDF-TrFE) as well as composite inks with reduced graphene oxide (PVDF-TrFE-rGO) were developed and adapted for continuous flow DIW. The composite PVDF-TrFE-rGO inks achieved percolation after 1.5 wt% and electrical conductivity of 2.8 S/cm at the highest loading investigate in this study (7 wt%). The inks were successfully printed with minimum nozzle diameter of 40 μm on different substrates including glass, metal and a nitrile elastomer. It was also demonstrated that the inks can be used to create a fully 3D-printed piezoelectric device with the predicted response, i.e. the fabrication technique did not deteriorate the functionality of the device. The conductive composite ink was successfully utilized as an effective electrode in the device. It was therefore demonstrated that by combining materials, such as the composite PVDF-TrFE-rGO ink and the *co*-polymer PVDF-TrFE with additive manufacturing techniques, the fabrication of low-cost, versatile devices can be achieved.

1. Introduction

Additive manufacturing (AM), commonly referred to as 3D-printing, is becoming an important addition to the toolbox of microsystems technology, as it can offer new levels of complexity while minimizing the fabrication steps required. It also widens the choice of materials that can be used for fabrication and as substrates. Simultaneous advances in fabrication techniques and material development have enabled the adoption of such technologies in biomedical engineering, with a broad spectrum of applications such as health monitoring, stimulating tissue growth, diagnostics and more [1–3]. Such applications impose further requirements on these devices such as mechanical flexibility, structural complexity and biocompatibility.

Many polymers are well suited for additive manufacturing techniques as well as for certain biomedical applications as they may be made flexible and biocompatible. Some are also piezoelectric, a property used in sensing or actuating applications. For example, PVDF is a polymer which is widely considered to be biocompatible and can be polarized with an external electric field and give a piezoelectric effect [4,5]. PVDF *co*-polymers, such as PVDF-TrFE have also been developed, to favour direct crystallization in the piezoelectric β phase due to the extra fluorine atom in each repeating unit [6,7]. The stretching which normally is required to achieve the β-phase in PVDF is then avoided, making the *co*-polymer more suitable for AM. PVDF-TrFE has already been used in microsystems technology, but commercially available inks are not adapted for additive manufacturing [8].

Most polymers are insulating materials which limits their incorporation in devices where conductivity is required. Various approaches have been implemented to obtain conductive polymers, e.g. by incorporating different additives such as metal nanoparticles and carbon-based materials [9–13]. Graphene materials have attracted significant attention in the last decade as conductive fillers. Specifically, reduced graphene oxide (rGO) is an excellent conductive filler for polymeric matrices since it has high electrical conductivity, as well as a large surface area, which enables percolation at much lower concentrations compared to metals and other carbon derivatives, thus maintaining the flexibility of the polymer matrix.

There are various 3D printing techniques available today. One of the most versatile and well-suited techniques for microfabrication is direct ink writing (DIW). DIW is a technique where an ink is deposited through

* Corresponding author at: Division of Microsystems Technology, Department of Materials Science and Engineering, Uppsala University, Uppsala 751 05, Sweden.
E-mail address: antrea.spanou@angstrom.uu.se (A. Spanou).

https://doi.org/10.1016/j.mne.2023.100190
Received 15 December 2022; Received in revised form 11 April 2023; Accepted 22 April 2023
Available online 25 April 2023

a nozzle system in a computer- controlled pattern, layer by layer, defining the resulting solid 3D structure [14]. DIW systems are versatile in setup and can be categorized into two basic types: ink- jet printing and continuous flow [14]. For the former, the ink is deposited drop by drop, whereas for the latter the ink is continuously dispensed from the nozzle and the dispensed strand is deposited on the platform/printed structure based on a determined pattern [3]. Direct ink writing is well suited for a wide variety of materials [3].

Fully 3D printed polymeric devices, combining conductive polymeric inks and piezoelectric polymeric inks poses several advantages. For example, the ability to print both the active material and the electrodes using the same process is both time and cost effective, as cleanroom techniques are not necessary. This means that fast design iterations are also feasible. One of the most important advantages for actuator structures is that the combination allows for easier fabrication of multilayered structures, where a lower operation voltage can be used [8]. This is an important parameter for the adoption of such devices in microsystems for biomedical applications.

In this work PVDF-TrFE and PVDF-TrFE-rGO inks suitable for continuous flow DIW were developed. The versatility of these inks combined with DIW was demonstrated by fabricating fully 3D -printed, polymer based functional piezoelectric devices. The potential for fabrication of biomedical devices in low-cost settings, with minimal fabrication and post processing steps can then be realized.

2. Materials and methods

2.1. Ink preparation

A reference PVDF-TrFE ink was prepared by sonicating PVDF-TrFE powder (Piezotech FC20, Arkema, France) in methyl-ethyl-ketone (MEK) (Sigma Aldrich, Germany), for 1 h. The composite PVDF-TrFE-rGO inks were prepared using reduced graphene oxide (Graphmatech, Sweden). Reduced graphene oxide was chosen after preliminary studies which showed better compatibility with the chosen polymer matrix than other graphene types. First an appropriate amount of graphene was dispersed in MEK using sonication for 1 h. Then the polymer powder was added and sonicated for 1 h, followed by 10 min of high sheer mixing (Fisherbrand 850 Homogenizer, Fisherbrand, Sweden). Different concentrations of composite inks were prepared (0.5, 1, 1.5, 2, 2.5,3,5 & 7 wt% relative to the dry mass).

2.2. Rheological properties of the inks

The rheological properties of the inks with the best preliminary printing results, were determined using flow sweep measurements in a shear rate range of 0.1 s^{-1}–100 s^{-1} (HR10 Rheometer, TA instruments, USA). A parallel plate geometry was used with 12 mm diameter. The loading gap was 1000 μm and the trip gap was 50 μm. The equilibration time was 5.0 s, the averaging time 30.0 s and no soak time was used to prevent setting of the ink during the measurement. The rheological properties of the manufactured inks were compared to a commercial PVDF-TrFE ink (Ink P, Arkema, France).

2.3. Determining the electrical conductivity

The electrical conductivity of the inks with different concentrations were determined using four-point probe measurements (CMT-SR2000N, AIT, South Korea). The inks were transferred to glass slides manually using a pipette, to create 20 × 30 mm rectangular films, with 30 μm resulting thickness. The sheet resistance and volume resistivity were measured.

2.4. Fabrication system

An in-house continuous flow DIW printer was used for manufacturing of the polymer devices (See Fig. 1). The ink was loaded in an airtight syringe, and extruded though a nozzle by a piston. The piston movement is controlled by a linear piezoelectric motor (Piezomotor LTC2013) which in return is controlled by a computer program. The flow speed to extrude the ink can be varied continuously between 0.25 and 7500 pl/s. In this system, two different nozzles were used. For structures above 100 μm a metal nozzle with inner diameter of 180 μm was used whereas for structures smaller than 100 μm glass nozzles with nozzle inner diameter of 40 μm were prepared. The glass nozzles were prepared by pulling glass capillaries with a capillary puller (P-1000, Sutter instrument, USA), scoring, and then cutting to the desired diameter. The pattern is determined by a computer program (LABVIEW, National instruments, USA) which drives the build plate, where the substrate is attached, in x-y-z directions.

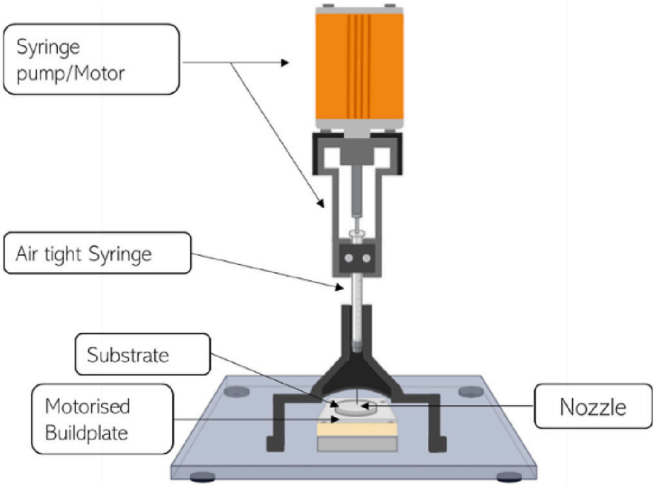

Fig. 1. a schematic of the DIW system. A computer-controlled 3-axes motorized table allows sub-micrometer positioning resolution of the substrate on a buildplate. The print head consists of a syringe pump directly driving the piston of an air tight syringe. Typically, the nozzle is the tip of a metal needle attached to the syringe. (to be printed in colour).

2.5. Morphological characterization

The morphology of the resulting structures was examined by scanning electron microscopy (SEM) (Zeiss Leo 1530, Carl Zeiss, Germany). An acceleration voltage of 3 kV was used and the samples were sputtered with Au—Pd prior to imaging. For the cross-sectional images, the polymer structures were cooled in liquid nitrogen before snapping, to obtain a cross section. The thickness was evaluated using both cross-sectional SEM images as well as a length gauge (Heidenhain, Germany). The length gauge probe has a rounded tip stylus and exerts a force of 0.7 N.

2.6. Piezoelectric device fabrication and characterization

The piezoelectric device was 3D printed using the composite 5 wt% rGO ink as the electrode material and the reference PVDF-TrFE ink as the active material, see 2.1. All layers were printed with lateral dimensions and patterns indicated in Fig. 2 using a metal 180 μm nozzle. First the composite ink was printed on a piezoceramic substrate. Then seven subsequent layers of the reference ink were printed in alternating printing orientation between each layer, with a final layer of composite ink printed on top. The reference P(VDF-TrFE) ink was printed with a pitch between printed lines equal to the observed strand width (270 μm) to create a homogeneous film.

A polarized piezoceramic substrate (Dongil Technologies, South Korea) of 16 mm diameter and 0.5 mm thickness with silver electrodes on both sides was used as the substrate for driving the device during

characterization. A common ground for both components is ensured by printing the polymeric device on the negative side, connected to ground, of the piezoceramic. The positive side of the piezoceramic is connected to a power supply, where the input signal is fed. The input signal is controlled using a waveform generator (Syscomp, Canada), where a sinusoidal signal will be amplified by an amplifier (Physik Instrumente, Germany) to 0–100 V at different frequencies; 10 Hz, 100 Hz, 1 kHz. The output signal is measured from the top electrode of the printed device, using an oscilloscope (Picoscope, UK), where the probe (MI007) has a resistance of 1Mohm and a capacitance 57 pF. The impedance of the device was measured with a LCZ-meter (Keithley Instruments, USA).

3. Results and discussion

3.1. Rheological properties

As previously mentioned, PVDF- TrFE inks for sensor and actuator fabrication are commercially available, but they are not adapted for additive manufacturing. The viscosity of the ink is an important parameter to consider to enable high-quality printing, especially when developing composite inks. It is important to avoid poor dispersion of solid nanoparticles in viscous matrices as well as agglomerations, which can be detrimental when printing with a few micrometer opening nozzles. Therefore, it was necessary to develop tailored DIW inks, both PVDF-TrFE, used as our reference, and PVDF-TrFE- rGO composites. After visual and morphological inspection of the prints, the rheological properties of the reference and composite inks with the best printing results were examined and compared to the properties of a commercially available PVDF-TrFE ink (Fig. 3a). The commercial ink did not exhibit shear thinning behavior in the flow sweep examined range 0.1–100 s^{-1}, and maintains a high viscosity at 100 s^{-1}. The reference ink has a significantly lower viscosity of 1 Pa.s and a shear thinning trend is observed, but there is large variations between measurements. Only the composite ink exhibits shear thinning properties. Shear thinning has been considered as an important parameter for continuous filament DIW, where it has been suggested that there needs to be sufficient reduction of viscosity under the applied shear stress so the ink flows when pressure is applied during printing but can recover and maintain its structure when deposited on the print plate [3,11,14]. However, in the present study shear thinning is not a prerequisite since thin film layers are required. Lateral spreading is thus desired, and this can be controlled by ink rheology in combination with the printing parameters (Table S1.1 & S1.2). Here, it is most important that the viscosity of the ink is well tuned with the evaporation of the solvent to result in the desired structures. The addition of rGO increases the viscosity of the ink, due to the increased overall dry mass of the same [11]. Possibly, rheological changes due to higher ink flow rates results in favorable conducting paths in the composite.

3.2. Conductivity

Composite inks were prepared with different concentrations to determine the percolation threshold and conductivity curve of the PVDF-TrFE-rGO inks. The results from the four-point probe measurement can be seen in Fig. 3b. The percolation point was after 1.5 wt% and the maximum conductivity recorded was 2.8 S/cm at the maximum loading tested (7 wt%). The percolation point for electrical conductivity in polymers is highly dependent on the dispersibility of the conductive filler in the matrix, as well as compatibility of the filler with the matrix. Cross-sectional images of the films with a filler concentration at the percolation threshold, reveal good dispersibility, yet partial agglomeration is still observed. (Fig. 3d - e) Fig. 3e indicates good interaction between the rGO flakes and the surrounding matrix despite the agglomeration. The percolation point achieved is comparable to other studies of carbon derivatives, however the highest value of conductivity achieved is higher than in the reported studies [9,11]. It is important to mention that higher conductivities have been reported using direct ink writing, with graphene based DIW inks [10,12]. However, post processing such as sintering or annealing of the polymer matrix is required to achieve these values, thus increasing the fabrication steps required and sacrificing the 3D capabilities.

Table 1
Comparison with current state of the art conductive inks for DIW.

Product/Study area	Conductivity	Comparison to present study	Reference
Present study	>1 S/cm	–	–
Carbon – polymer based inks for DIW [5,7]	~1 S/cm	Comparable studies exhibit same percolation but lower maximum conductivity	[9,11]
PEDOT:PSS [15]	<1 S/cm	Lower conductivity than present study	[15]
Doped PEDOT:PSS [15]	>100S/cm	Need to use strong acids/toxic solvents to achieve high conductivity PEDOT:PSS. IT is substrate specific.	[15]
Graphene - inks for inkjet printing [10,12]	~1 S/cm, >100 S/cm	Higher conductivity can be achieved but requires post processing (annealing/ sintering) – limitation in 3D configurations	[10,12]
Metal based inks [13]	>100 S/cm	Higher conductivity but lower printing resolution than current study	[13]

Table 2
Layer thickness based on printing parameters for reference PVDF-TrFE inks.

Ink type	Gap distance (um)	Flow rate (pL/s)	Layer thickness (μm)
Ref. PVDF-TrFE	30	2000	1.9±0.2
Ref. PVDF-TrFE	60	4000	3.9±0.2
Ref. PVDF-TrFE	90	6000	5.9±0.2

Compared to other state-of-the-art conductive inks for DIW the presented approach possesses several advantages (Table 1). For example, the electrical conductivity of as-cast conductive PEDOT:PSS does not exceed 1 S/cm. When comparing polymer-graphene composites with doped PEDOT:PSS that have significantly higher conductivity, there are other limitations. Doping of PEDOT:PSS involves strong acids or toxic solvents, which requires special handling conditions [15]. In addition, the acidity of the system and the ability of the PSS to diffuse in other components, can lead to deterioration of the device due to side reactions, which raises questions regarding device stability and integration [15]. In this work, the solvents used are benign and a major requirement of the fabrication process is that the solvent can easily evaporate from the system to achieve solid structures. It is thus a better alternative for applications where ease of handling is important and toxicity problems can become an issue. Polymer-graphene composites have a significant advantage over metal-based inks since graphene is chemically stable and can withstand humid environments. This makes handling during fabrication easier and broadens the applications for flexible devices using this composite electrode.

3.3. Printability

The inks were printed using continuous flow direct ink writing. First a metal 180 um nozzle was used to print both reference PVDF-TrFE and 5 wt% PVDF-TrFE-rGO composite inks. In both cases the printed structures had good continuity, uniformity, and lateral shape control. The composite ink resulted in rougher surface due to the rGO (Fig. 4 c). Similar morphologies have been observed elsewhere, where carbon fillers have been incorporated into the polymer matrix [11]. A pattern according to Figs. 4 e-g was printed with the composite ink, to demonstrate the versatility of the fabrication technique. The resulting thickness

Table 3
Comparison of DIW nozzle diameter with conductive inks.

Matrix	Conductive filler	Min. nozzle diameter (μm)	Ref.
PVDF-TrFE	rGO	40	Present study
Poly (D,L-lactide-*co*-trimethylene carbonate)	CNT	200	[11]
Ethylene glycol	CNT	60	[19]
PEDOT:PSS	–	30	[20]
TPU	Ag	200	[13]

of a single layer of the reference ink can be varied between 2 and 6 um using the 180 um nozzle (Table 2). This is tuned by selecting the gap between the nozzle and the print plate in combination with an appropriate flow rate.

When introducing conductive fillers to a polymer matrix, one major challenge in DIW is the achievable detail resolution, which is closely related to the nozzle diameter. The minimum nozzle size that can be used is typically significantly larger than those used for the pure polymers, as there is higher risk of clogging. There are two parameters that have been observed to influence clogging – the degree of agglomeration of the fillers and the size of the filler particles. Based on preliminary work outcomes (Fig. S2) the most compatible graphene type, reduced graphene oxide, was chosen to promote dispersion in the matrix and minimize agglomeration. It is worth mentioning that several functionalization techniques, to improve flake separation of the graphene and dispersibility of graphene in polymers, have been employed elsewhere [9,16]. Even though functionalization improves dispersion of graphene in polymer matrices, functionalization comes at the cost of conductivity. This is because the functional groups that prevent the re-stacking [17], and thus the agglomeration of the graphene flakes, also obstruct the in-plane conduction of π-electrons [17,18]. In this case, the reduced graphene oxide flakes appear to have sufficient compatibility with the polymer matrix to avoid large agglomerations and achieve good dispersion, even though small agglomerations are not entirely eliminated. It was therefore decided to proceed with non-functionalized rGO, and test whether the highly conductive inks are printable with a nozzle diameter below 100 μm. The 5 wt% PVDF-TrFE-rGO inks were successfully printed with a nozzle size of 40 μm diameter (Fig. 4d). This is better than what has been reported in other studies using carbon-based fillers, and comparable with the state of the art regarding DIW of conducting polymers (Table 3). Here the flow was gradually decreased during the print from 2000 to 1000 pl/s. At 1000 pl/s, there is still over-extrusion and thus the strand width was larger than the diameter of the nozzle. Lower flow rates and gap distance can be used to achieve 40 μm features. However, this would increase the resistance of the single print layer, as the thickness would decrease to below 1 μm. This can be solved by printing multiple conductive layers. Here it is demonstrated that highly loaded graphene inks can be printed with nozzles below 100 μm and that different features can be obtained within the same layer by tuning different printing parameters.

Another advantage of AM in microsystems technology is that non-specialized substrates can be used for fabrication. This is particularly important regarding sensor integration on non-conventional surfaces. The inks were successfully printed on different substrates including metal coated ceramic substrates, glass, nitrile gloves and metal

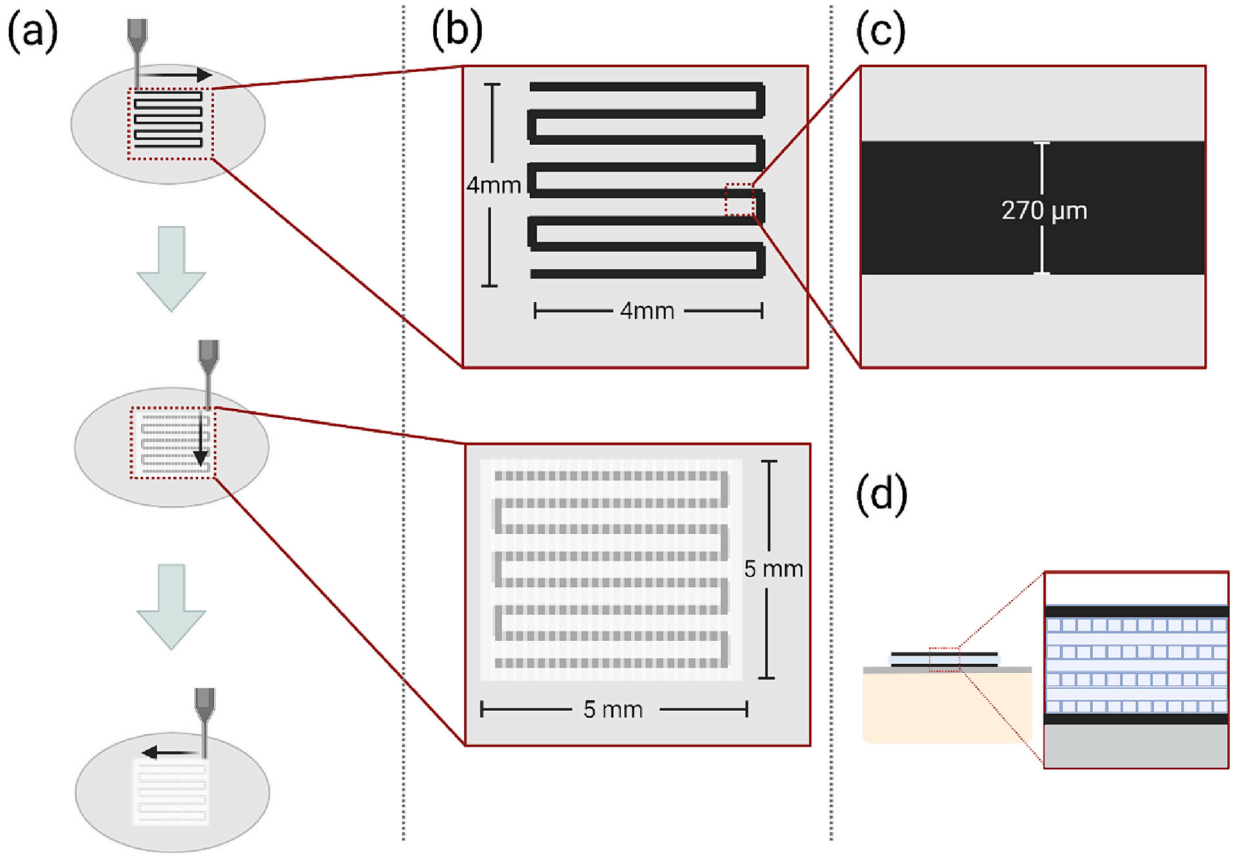

Fig. 2. Illustration of the fabrication method: (a, top) the composite ink is first printed on the piezoceramic substrate's electrode in the indicated pattern followed by (a, middle and bottom illustrations) reference ink layers in alternating printing directions for each layer (indicated by the black arrows); (b) lateral dimensions of the different print layers, the top image depicting the electrode dimensions and the bottom image depicting the first active layer being 0,5 mm larger on each side to ensure coverage and prevent contact between top and bottom electrodes; (c) strand width of printed electrode; (d) cross-section of the printed device on the piezoceramic substrate with 7 reference PVDF-TrFE layers in alternating directions and two (top and bottom) electrodes (to be printed in colour).

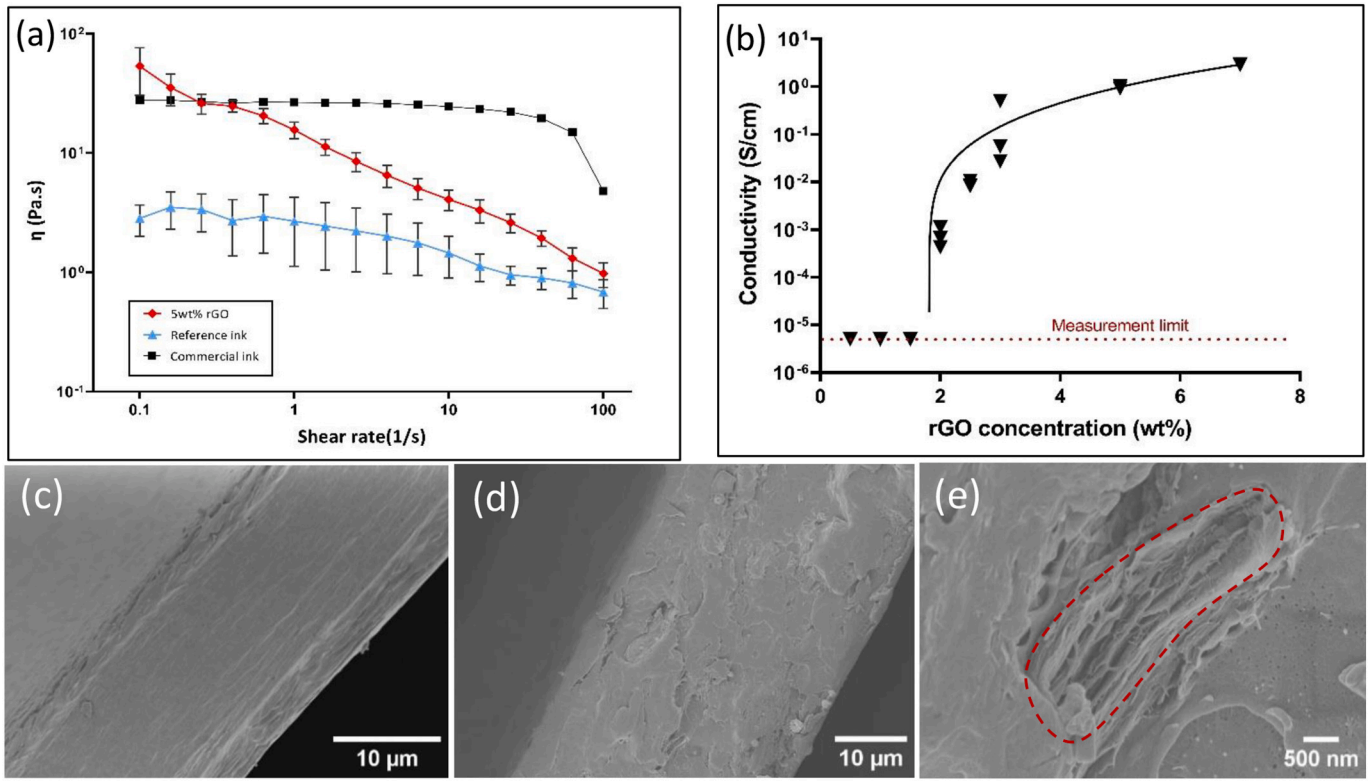

Fig. 3. Ink characterization: (a) apparent viscosity vs shear rate; (b) electrical percolation curve (three measurements are presented per concentration, nonlinear regression curve fit is used); (c-e) cross section images of cast films: (c) reference PVDF-TrFE ink, (d - e) 1.5 wt% PVDF-TrFE- rGO ink demonstrating a fair dispersion with occasional agglomerations (e) indicated in the red dashed border. The agglomerations have a stacking thickness of about 1 μm or less. (to be printed in colour). (For interpretation of the references to colour in this figure legend, the reader is referred to the web version of this article.)

substrates (Fig. 4 e-g). The prints on all substrates withstood the friction caused by the normal force exerted by the Heidenhain probe, during lateral movement under the probe, which could be interpreted as sufficient adhesion for several applications.

3.4. Piezoelectric device

To demonstrate the possibilities with these inks, a fully 3D printed polymer-based device was fabricated. The device was printed on a piezoceramic substrate and consisted of 9 layers in total, 2 electrodes (top and bottom) made of the 5% PVDF-TrFE-rGO ink. The reference PVDF-TrFE ink was used as the active material of the device. The electrodes printed with the composite conductive ink, had a pattern according to Fig. 2, to evaluate the printing possibilities and limits. As can be seen in Fig. 4e-g it is possible to print electrical patterns on various substrates and the present minimum width is 40 μm. It would thus be possible to, for instance, print piezoresistive strain gauges with sub-millimeter dimensions. When printing piezoelectric components, a good interface needs to be established between the electrode and the active material. In this case we expect good interaction between the electrode layers and the active material layers, since the same polymer matrix is used (Fig. 5a). What is also interesting to observe is that an excellent interlayer adhesion was achieved between the layers of the reference ink with no sign of print lines from previous layers. This likely depends on a slight fusion between the previous and the subsequent layer, before the latter sets. However, this does not come at the cost of disrupting the spatial arrangement of each feature, as distinct print regions of each strand are observed in the top view of the device (Fig. 5b). A good interlayer adhesion and fusion is important for the piezoelectric device, so that the risk for electric breakdown is minimized.

The device was polarized (Fig. S3 - a) and then evaluated as a sensor film. This was done by driving the piezoceramic substrate, whose strain can be calculated from the material d_{13} piezoelectric coefficient at quasi-static frequencies, and recording the response from the printed device. The strain of the printed device in the lateral directions will be equal to the strain in the substrate (Fig. S3-b). The substrate was driven at different frequencies within the quasi-static regime and the relationship was established between the driving signal of the substrate and the measured signal of the 3D printed device. As long as the substrate is driven in the quasi-static regime, the generated signal from the printed device (V_p) in ideal conditions, will be in phase with the driving signal of the piezoceramic substrate (V_{in}). The capacitance of the sensor film was 35 pF at 120 Hz and including the impedance of the oscilloscope used for the measurements we can model the electrical behavior as an R-C circuit according to Fig. 5f. The derivation of this model is described in more detail in the supporting information S3. Here $R_m >> R_p$, where R_m is the resistance in the measurement probe and R_p is the resistance in the printed device, thus R_p has minimal influence in output voltage signal (V_{out}). For low frequencies, a 90° phase shift between V_{in} and V_{out} as well as a linear amplitude increase of V_{out} with frequency is expected due to the oscilloscope impedance. This is in accordance with the observed results at 10–100 Hz (Fig. 5d-e). At 1 kHz a 53° phase shift between the drive signal of the piezoceramic and the output signal of the printed device is observed, Fig. 5c. This phase shift agrees reasonably well with calculations using the R-C-model including the capacitance of the oscilloscope probe, where a theoretical phase shift of 56° is calculated. The expected amplitude increase with frequency in the range 100–1000 Hz will be lower (~10%) than in the range 10–100 Hz, which agrees well with Fig. 5e.

The performance of the top printed electrode was also evaluated. This was done by comparing the calculated expected capacitance of the device and the measured capacitance. The relative permittivity of the polymer, provided by the manufacturer, is 9 measured at 1 kHz. The calculated capacitance, when considering the electrode configuration

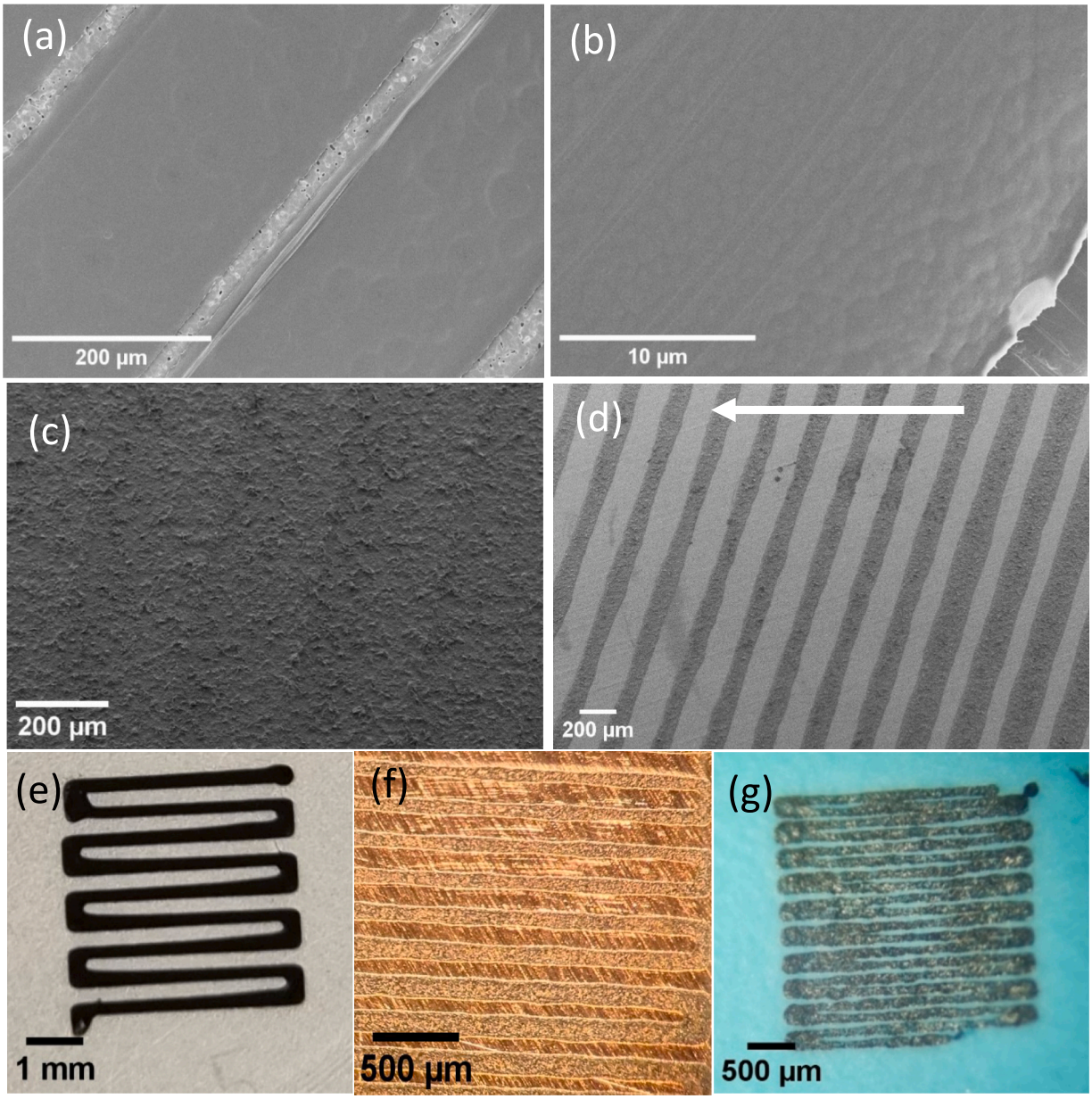

Fig. 4. Visualization of 3D printed inks. (a-b) PVDF-TrFE reference with a) visible grooves between print lines and b) a magnification of the printed surface. (c) 5 wt % PVDF-TrFE-rGO (a-c) printed with 180 µm nozzle (d) 5 wt% rGO printed with 40 µm nozzle. The dark grey is regions of printed ink and the light grey regions the substrate. The direction of the decreasing flow rate is indicated by the white arrow. Printing on different substrates is illustrated in (e-g): (e) substrate: metal coated piezoceramic (f) substrate: copper (g) substrate: nitrile glove. (e-f) printed with 40 µm nozzle. (to be printed in colour).

used (Fig. 2) and a device thickness of 20 µm, is 37 pF. At 1 kHz the measurements gave a capacitance of 35 pF and a phase angle of 88.9°, therefore the electrode performance can be considered satisfactory.

Here it is demonstrated that both conductive and piezoelectric materials can be printed layer by layer in a straightforward manner, thus making it possible to print devices with multilayered electrodes. A potential advantage of this is that piezoelectric devices can be driven at reduced voltage. [8] This enables printable sensors and actuators, with unique morphologies and functionalities, at reduced costs and increased accessibility, as the need of cleanroom facilities would not be required.

4. Conclusions

In this work it has been demonstrated that piezoelectric PVDF-TrFE inks and composite PVDF-TrFE-rGO inks can be utilized for additive manufacturing of polymeric devices. The composite inks achieved a percolation threshold for concentrations comparable to what has been reported elsewhere when utilizing carbon fillers, yet a higher electrical conductivity is reported herein. The composite inks are sufficiently conductive to be used as effective electrodes but are not limited to this application. It is also demonstrated that the composite inks can be successfully printed with 40 µm nozzle diameter. Most importantly, it is demonstrated that by combining conductive and piezoelectric polymeric materials with additive manufacturing, fully printed devices which are not substrate dependent can be achieved. This can contribute to the development of sensors and actuators, with complex architectures and multilayered structure, which can broaden the possibilities in microsystem technology. Many developing application fields such as biomedical engineering could benefit from such materials and methods. The adoption of these techniques for low-cost settings, where cleanroom facilities are not always available, would also be realized.

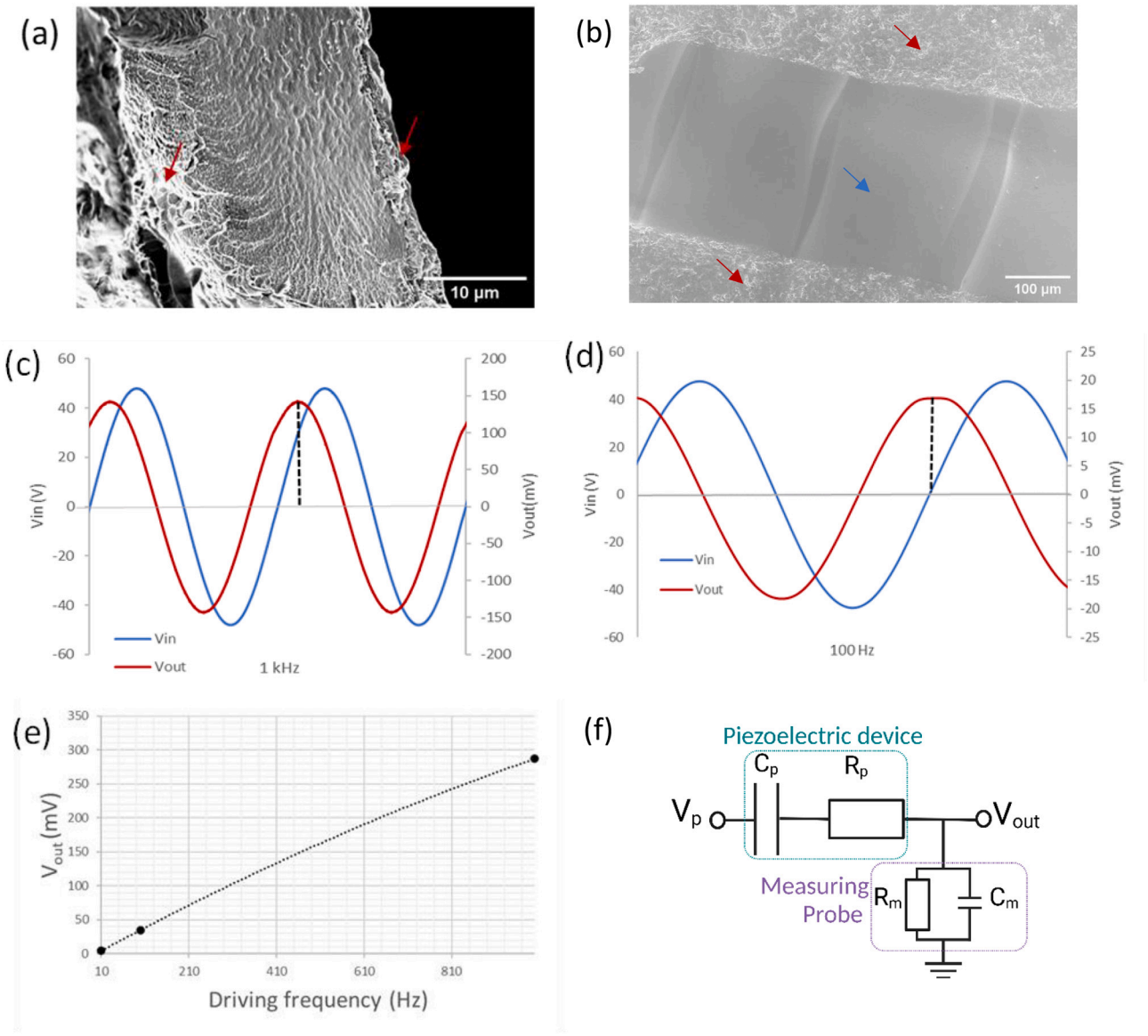

Fig. 5. Visualization and performance of the piezoelectric device: (a) cross-sectional SEM image of the piezoelectric printed device, the red arrows show the electrodes printed with the composite ink; (b) top view SEM image of printed piezoelectric device – the electrodes are indicated with the red arrows, and blue arrow indicates the active material; (c) output voltage at 1 kHz; (d) output voltage at 100 Hz; and (e) output peak-to-peak voltage – driving frequency relationship. Dotted line is the best fit second-degree polynomial (f) Equivalent circuit diagram, where C_p and $R_{p,}$ are the capacitance and resistance respectively of the printed device and R_m and C_m are the resistance and capacitance respectively of the measuring probe, V_p is the generated voltage signal in the piezoelectric device, and V_{out} is the output voltage signal detected by the oscilloscope (to be printed in colour). (For interpretation of the references to colour in this figure legend, the reader is referred to the web version of this article.)

Funding

This work is conducted within the Additive Manufacturing for the Life Sciences Competence Center (AM4Life). The authors gratefully acknowledge financial support from Sweden's Innovation Agency VINNOVA (Grant no: 2019-00029).

Declaration of Competing Interest

The authors declare the following financial interests/personal relationships which may be considered as potential competing interests:

Cecilia Persson reports financial support was provided by Sweden's Innovation Agency. Antrea Spanou reports financial support was provided by Graphmatech.

Data availability

Data will be made available on request.

Acknowledgements

Myfab Uppsala is acknowledged for access to the scanning electron microscope. The authors would like to acknowledge Christos Leliopoulos for providing training on how to conduct the rheological measurements and providing insights into the techniques. It is also acknowledged that the creation of some graphical artwork has been facilitated by biorender.com.

Appendix A. Supplementary data

Supplementary data to this article can be found online at https://doi.org/10.1016/j.mne.2023.100190.

References

[1] S. Azimi, A. Golabchi, A. Nekookar, S. Rabbani, M.H. Amiri, K. Asadi, et al., Self-powered cardiac pacemaker by piezoelectric polymer nanogenerator implant, Nano Energy 83 (2021 May 1).

[2] F. Mokhtari, B. Azimi, M. Salehi, S. Hashemikia, S. Danti, Recent Advances of Polymer-Based Piezoelectric Composites for Biomedical Applications vol. 122, Elsevier Ltd, 2021. Journal of the Mechanical Behavior of Biomedical Materials.

[3] P. Jiang, Z. Ji, X. Zhang, Z. Liu, X. Wang, Recent advances in direct ink writing of electronic components and functional devices, in: Progress in Additive Manufacturing vol. 3, Springer, 2018, pp. 65–86.

[4] O. Gryshkov, F. Al Halabi, A.I. Kuhn, S. Leal-Marin, L.J. Freund, M. Förthmann, et al., Pvdf and p(Vdf-trfe) electrospun scaffolds for nerve graft engineering: a comparative study on piezoelectric and structural properties, and in vitro biocompatibility, Int. J. Mol. Sci. 22 (21) (2021 Nov 1).

[5] Y. Yu, H. Sun, H. Orbay, F. Chen, C.G. England, W. Cai, et al., Biocompatibility and in vivo operation of implantable mesoporous PVDF-based nanogenerators, Nano Energy 27 (2016 Sep 1) 275–281.

[6] A.J. Lovinger, Ferroelectric polymers, Science 220 (1983) 1115.

[7] X. Zhou, K. Parida, O. Halevi, Y. Liu, J. Xiong, S. Magdassi, et al., All 3D-printed stretchable piezoelectric nanogenerator with non-protruding kirigami structure, Nano Energy 72 (2020 Jun 1).

[8] N. Snis, E. Edqvist, U. Simu, S. Johansson, Monolithic fabrication of multilayer P (VDF-TrFE) cantilevers, Sens. Actuators A Phys. 144 (2) (2008 Jun 15) 314–320.

[9] V. Sankar, V. Sankar, A. Nambi, V.N. Bhat, D. Sethy, K. Balasubramaniam, et al., Waterproof flexible polymer-functionalized graphene-based Piezoresistive strain sensor for structural health monitoring and wearable devices, ACS Omega 5 (22) (2020 Jun 9) 12682–12691.

[10] E.B. Secor, P.L. Prabhumirashi, K. Puntambekar, M.L. Geier, M.C. Hersam, Inkjet printing of high conductivity, flexible graphene patterns, J. Phys. Chem. Lett. 4 (8) (2013 Apr 18) 1347–1351.

[11] X. Wan, F. Zhang, Y. Liu, J. Leng, CNT-based electro-responsive shape memory functionalized 3D printed nanocomposites for liquid sensors, Carbon N. Y. 155 (2019 Dec 1) 77–87.

[12] A. Apostolakis, D. Barmpakos, A. Pilatis, G. Patsis, D.N. Pagonis, V. Belessi, et al., Resistivity study of inkjet-printed structures and electrical interfacing on flexible substrates, Micro Nano Eng. 15 (2022 Jun 1), 100129.

[13] A.D. Valentine, T.A. Busbee, J.W. Boley, J.R. Raney, A. Chortos, A. Kotikian, et al., Hybrid 3D printing of soft electronics, Adv. Mater. 29 (40) (2017 Oct 25).

[14] J.A. Lewis, Direct ink writing of 3D functional materials, Adv. Funct. Mater. 16 (17) (2006 Nov 3) 2193–2204.

[15] X. Fan, W. Nie, H. Tsai, N. Wang, H. Huang, Y. Cheng, et al., PEDOT:PSS for Flexible and stretchable electronics: Modifications, strategies, and applications, in: Advanced Science vol. 6, John Wiley and Sons Inc., 2019.

[16] D. Wang, Y. Bao, J.W. Zha, J. Zhao, Z.M. Dang, G.H. Hu, Improved dielectric properties of nanocomposites based on poly(vinylidene fluoride) and poly(vinyl alcohol)-functionalized graphene, ACS Appl. Mater. Interfaces 4 (11) (2012 Nov 28) 6273–6279.

[17] V.B. Mohan, R. Brown, K. Jayaraman, D. Bhattacharyya, Characterisation of reduced graphene oxide: effects of reduction variables on electrical conductivity, Mater. Sci. Eng. B Solid State Mater. Adv. Technol. 193 (C) (2015 Jul 1) 49–60.

[18] S.H.M. Jafri, K. Carva, E. Widenkvist, T. Blom, B. Sanyal, J. Fransson, et al., Conductivity engineering of graphene by defect formation, J. Phys. D. Appl. Phys. 43 (4) (2010).

[19] W. Yu, H. Zhou, B.Q. Li, S. Ding, 3D printing of carbon nanotubes-based microsupercapacitors, ACS Appl. Mater. Interfaces 9 (5) (2017 Feb 8) 4597–4604.

[20] H. Yuk, B. Lu, S. Lin, K. Qu, J. Xu, J. Luo, et al., 3D printing of conducting polymers, Nat. Commun. 11 (1) (2020 Dec 1).